

# $\pi$ -Conjugated Carbon Radicals at Graphene Oxide to Initiate Ultrastrong Chemiluminescence\*\*

Liang Yang, Ruilong Zhang, Bianhua Liu, Jianping Wang, Suhua Wang, Ming-Yong Han, and Zhongping Zhang\*

**Abstract:** Graphene oxide has widely been employed in various fields, but its structure and composition has still not been fully understood. Here we report that freshly prepared graphene oxide exhibits a large number of  $\pi$ -conjugated carbon radicals at its  $\pi$ -network plane, which result from the addition reaction of hydroxyl radicals from  $H_2O_2$  onto the conjugated double bonds of graphene oxide. The  $\pi$ -conjugated carbon radicals can directly initiate the long-lasting visible chemiluminescence of luminol, which is even stronger than that obtained when horseradish peroxidase and  $H_2O_2$  are used. Previously, graphene oxide was mainly reported to be a quencher of chemiluminescence instead. Remarkably, the reacted radicals can be regenerated, thereby enabling the repetitive initiation of chemiluminescence by re-treatment of graphene oxide. The results reported here provide a new understanding of the structure, properties, and applications of graphene oxide.

Graphene oxide (GO) is a two-dimensional derivative of exfoliated graphite oxidized under strong oxidizing conditions. It has prominent properties such as an  $sp^2$  planar structure, several nanometer thickness, a highly hydrophilic nature, and a high number of functional groups, which have been envisioned to greatly benefit a wide range of promising applications.<sup>[1,2]</sup> Due to their thinness, the GO nanosheets are excellent precursors for the preparation of conductive polymer nanocomposites,<sup>[3]</sup> very thin carbon films,<sup>[4]</sup> and carbonaceous electronic circuits.<sup>[5]</sup> Because of the hydrophilic properties and surface groups, GO has also been used for molecular recognition and detection and as an ink to print paper-based chemosensors.<sup>[6]</sup> Modification of the surface

groups of GO result in photoluminescent,<sup>[7]</sup> adsorbent,<sup>[8]</sup> and catalytic<sup>[9]</sup> materials. These applications are based on the current knowledge of the structures and compositions of GO. However, the properties of GO are only poorly understood so far, limiting its use for other applications.

Although GO was first prepared 150 years ago,<sup>[10]</sup> its exact chemical structure is still ambiguous to date, and the reasons are given below. Firstly, a number of strong oxidants ( $P_2O_5$ ,  $H_2SO_4$ ,  $K_2S_2O_8$ ,  $KMnO_4$ , and  $H_2O_2$ ) is needed to synthesize GO, leading to a variety of possible compositions and structures. Secondly, unlike a molecule, it is a nonstoichiometric substance. Thirdly, it decomposes slowly at elevated temperature. Currently, there are several different structural models on the carbon skeletons and surface species of GO, which have been proposed by Hofmann,<sup>[11]</sup> Ruess,<sup>[12]</sup> Scholz,<sup>[13]</sup> Nakajima,<sup>[14]</sup> and Lerf<sup>[15]</sup> based on the analysis by IR, Raman, XPS, and NMR spectroscopy. Although these models reasonably interpret the individual physical properties such as the electric, reductive, and hydrophilic features of GO, they cannot provide an appropriate understanding of some experimental results. For example, as a strong quencher of fluorescence and chemiluminescence,<sup>[16]</sup> GO itself can also produce weak photoluminescence.<sup>[17]</sup> The comprised and widely accepted model is a disrupted planar  $\pi$ -network bearing the phenol hydroxy and epoxide groups at its basal plane and the carboxylic groups at its lateral edge. Here, we report a novel insight into the structure and properties of freshly-prepared GO, which has a large number of  $\pi$ -conjugated carbon radicals at the  $\pi$ -network plane. The carbon radicals exhibit strong oxidizing properties and directly initiate the strong chemiluminescence of luminol.

Figure 1 illustrates the four-step synthesis of GO by the classical Hummers method.<sup>[18]</sup> Graphite is first oxidized by  $P_2O_5$  and  $K_2S_2O_8$  (step 1); the resulting graphite oxide was then exfoliated and further oxidized to GO nanosheets by  $H_2SO_4$  and  $KMnO_4$  (steps 2 and 3), and finally the excess  $KMnO_4$  was removed by addition of  $H_2O_2$  (step 4). This classical four-step procedure led to the formation of the first product (GO-1). Using only steps 1–3 produced the second product (GO-2). After a thorough purification by centrifugation and washing with ultrapure water for several times, GO-1 and GO-2 were further dialyzed in iced water overnight to completely remove any residual impurities, followed by storage in water at 4 °C for use. Both, GO-1 and GO-2, were completely identical in appearance, and there were also no differences in chemical composition and structure as observed by atomic force microscopy, Raman spectroscopy, and infrared spectroscopy (Figure S1–S3). However, the GO-

[\*] L. Yang, R. Zhang, J. Wang, Prof. Z. Zhang  
Department of Chemistry  
University of Science & Technology of China  
Hefei, Anhui 230026 (China)  
E-mail: zpzhong@iim.ac.cn

L. Yang, R. Zhang, B. Liu, J. Wang, S. Wang, Dr. M. Han,  
Prof. Z. Zhang  
Institute of Intelligent Machines, Chinese Academy of Sciences  
Hefei, Anhui 230031 (China)  
Dr. M. Han  
Institute of Materials Research and Engineering  
A\*STAR, 3 Research Link  
Singapore 117602 (Republic of Singapore)

[\*\*] This work was supported by the National Key Technology R&D Program (Grant 2012BAJ24B02) and the National Natural Science Foundation of China (21335006, 21375131, 21275145, 21175137).

Supporting information for this article is available on the WWW under <http://dx.doi.org/10.1002/anie.201405295>.

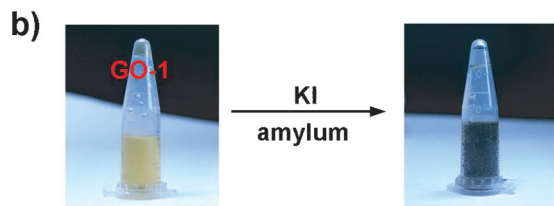
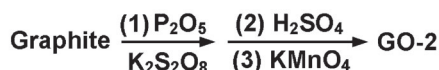
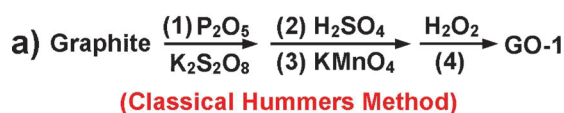


**Figure 1.** a) The classical three- or four-step synthesis of GO using graphite powder as the starting material. b) The purified GO-1 shows an obvious color reaction triggered by the addition of KI and amyllum.

1 compared to GO-2 showed a small blue-shift in the UV absorption spectra (at 225 and 230 nm, see Figure S4).

After the addition of KI and amyllum, surprisingly, the light yellow color of GO-1 solution immediately changed to deep blue (Figure 1b), whereas the light yellow color of the GO-2 solution remained unchanged. This shows that GO-1 can oxidize  $\text{I}^-$  ions into  $\text{I}_2$ , forming the blue triiodide-amyllum complex, whereas GO-2 cannot accomplish the reaction. This indicates that GO-1 itself can react with KI, because all oxidant residues, i.e.,  $\text{KMnO}_4$  and  $\text{H}_2\text{O}_2$ , were completely removed before. Thus we have reason to speculate that the addition of  $\text{H}_2\text{O}_2$  in the fourth step plays a role not only in removing the excess  $\text{KMnO}_4$  but also leading to a change of the composition and structure of GO-1, which renders the oxidative ability of GO-1. The oxidation equivalent of the GO-1 was then measured by iodometric titration (see the Supporting Information). After the reaction of GO-1 with KI, the resulting iodine was titrated with  $\text{Na}_2\text{S}_2\text{O}_3$  solution. The oxidation equivalent of GO-1 relative to  $\text{I}^-$  was evaluated to be  $2.18 \text{ mmol g}^{-1}$ , which was verified with a hydrazine test because hydrazine could also react with GO-1.

With the capability of capturing electrons and radicals with its  $\pi$ -conjugated aromatic plane, GO has been widely regarded as an effective quencher of fluorescence and chemiluminescence.<sup>[16]</sup> Similarly, we did not observe any chemiluminescence of luminol initiated by freshly prepared GO-2 solution. However, when luminol was added to the freshly prepared GO-1 solution, a very strong blue chemiluminescence was directly observed by the naked eye, which lasted for 18 s (Figure 2a). For a comparison, the chemiluminescence of GO-1 and GO-2 were measured as a function of time under identical conditions (Figure 2b). The optimal concentrations of GO-1 and luminol for initiating the strongest chemiluminescence were  $0.24 \text{ mg mL}^{-1}$  and  $1 \times 10^{-3} \text{ M}$ , respectively (Figure S5). These concentrations were used for all the following experiments.

The GO-1 can directly trigger the chemiluminescence of luminol without the need of additional oxidizing agents. Usually,  $\text{H}_2\text{O}_2$  and  $\text{KMnO}_4$  are used for this purpose. The

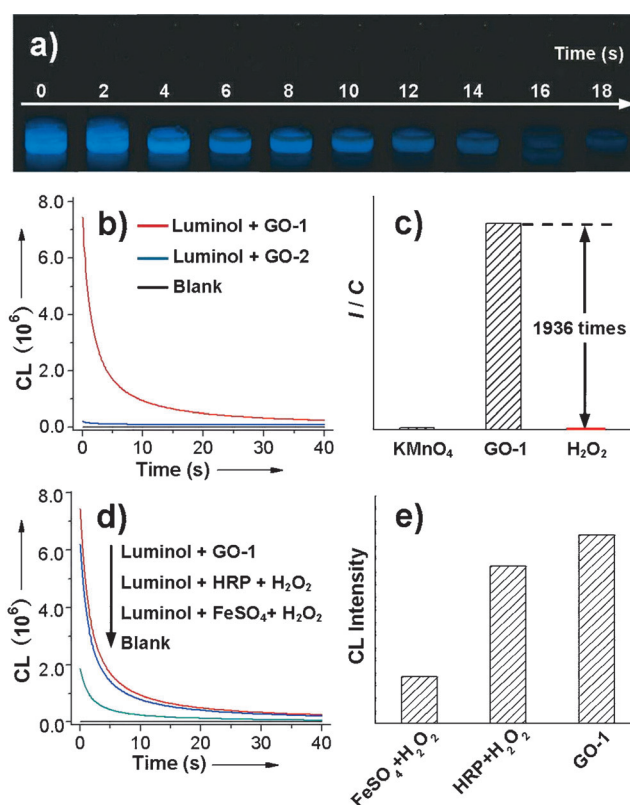


**Figure 2.** a) The strong and long-lasting visible chemiluminescence produced by the addition of luminol to a GO-1 solution. b) The chemiluminescence produced by the addition of luminol to a GO-1 solution, a GO-2 solution, and water as control. c) The comparison of the chemiluminescence efficiency of GO-1 with  $\text{KMnO}_4$  and  $\text{H}_2\text{O}_2$  ( $I$  is the chemiluminescence intensity;  $C$  is the molar concentration of oxidants). d) The chemiluminescence produced by the addition of luminol to GO-1, to a mixture of HRP ( $0.24 \text{ mg mL}^{-1}$ ) and  $\text{H}_2\text{O}_2$ , and to a mixture of  $\text{FeSO}_4$  ( $0.24 \text{ mg mL}^{-1}$ ) and  $\text{H}_2\text{O}_2$ . e) The comparison of chemiluminescence intensities in (d). It has to be noted that  $50 \mu\text{L}$  of  $1 \times 10^{-3} \text{ M}$  luminol at pH 13 was used for all above-shown experiments.

intensity of the chemiluminescence initiated by GO-1 was much stronger than those triggered by  $\text{H}_2\text{O}_2$  and  $\text{KMnO}_4$  (Figure S8), and calculated to be 1936 and 100 times more efficient, respectively (Figure 2c). This is further evidence that the ultrastrong chemiluminescence by GO-1 cannot be caused by residues of  $\text{H}_2\text{O}_2$  and  $\text{KMnO}_4$  in the sample.

So far, the strongest chemiluminescence was obtained by employing horseradish peroxidase (HRP) or Fenton agent ( $\text{FeSO}_4 + \text{H}_2\text{O}_2$ ); in both reactions, highly active radical intermediates play a key role in oxidizing luminol.  $\text{FeSO}_4$  can catalyze the decomposition of  $\text{H}_2\text{O}_2$  to produce strongly oxidizing hydroxyl radicals ( $\cdot\text{OH}$ ). Here, the ability of GO-1 to trigger the chemiluminescence of luminol was compared with the two systems  $\text{HRP} + \text{H}_2\text{O}_2$  and  $\text{FeSO}_4 + \text{H}_2\text{O}_2$ , using the same mass concentration of GO-1, HRP, and  $\text{FeSO}_4$  (Figure 2d). The results show that the chemiluminescence initiated by GO-1 is still much stronger than those initiated by HRP and  $\text{FeSO}_4$  (Figure 2e). The ultrastrong chemiluminescence indicates that GO-1 may exhibit strongly oxidizing species like radicals. It has to be noted that the chemiluminescence-initiating capability of GO-1 is retained in solution

at 4 °C for three days and subsequently attenuates with time (Figure S9).

In general, GO has been recognized to have a disrupted planar  $\pi$ -network structure, which exhibits phenol hydroxy and epoxide groups at the basal plane and carboxylic groups at the lateral edge. However, the  $\pi$ -network plane and its functional groups cannot provide a reasonable explanation for the origin of the oxidizing activity and ability to trigger the ultrastrong chemiluminescence of luminol. There are three major reasons that let us consider the presence of active radicals at GO-1: 1) the ultrastrong chemiluminescence of luminol, which is similar to that observed with HRP and usually related to radicals; 2) the gradual disappearance of the oxidizing capability in solution under air, which is a common feature of active radicals; and 3) the addition of  $\text{H}_2\text{O}_2$  in the fourth step of the GO synthesis that renders the ability to trigger the chemiluminescence of luminol. In fact, HRP first reacts with  $\text{H}_2\text{O}_2$  to form  $\pi$ -conjugated radicals, which oxidize luminol, causing strong chemiluminescence.<sup>[19]</sup>

Electron paramagnetic resonance (EPR) is a sensitive and specific technique for studying the radicals formed in chemical reactions. As shown in Figure 3a, GO-1 displays a very sharp and intensive resonance peak with  $g = 2.003$ . The high intensity and very narrow width of this peak imply that there are no conduction carriers in the GO-1 nanosheets, unlike graphite.<sup>[20]</sup> Namely, GO-1 does not have highly extended aromatic planes, and the presence of many aromatic rings, disrupting the planes, avoid the formation of a conduction band. The origin of the spin species can be clarified by considering the EPR spectrum of GO-2, which did not exhibit any EPR signal. Therefore, the EPR signal of GO-1 does not result from the mobile  $\pi$  electrons at aromatic rings, but from the possible radical species produced after the chemical treatment with  $\text{H}_2\text{O}_2$ . Further evidence was obtained by mixing  $\text{H}_2\text{O}_2$  and GO-2, which produced a weak EPR signal with an identical  $g = 2.003$ , whereas individual  $\text{H}_2\text{O}_2$  did not give any EPR signal (Figure 3b). Therefore, the addition of  $\text{H}_2\text{O}_2$  in the synthesis of GO-1 led to the appearance of the EPR signal.

On the other hand, the EPR signal of GO-1 gradually disappeared after the addition of KI to GO-1 or the thermal treatment of GO-1 at 60 °C (Figure 3c,d). This suggests that GO-1 contains the oxidizing radicals, which can react with KI or quench themselves in solution under air and at elevated temperatures. It is well known that  $\cdot\text{OH}$  radicals are highly instable and do not exist in aqueous solution or under air. Accordingly, all presented results, together with the  $g$  value, allow the final conclusion that the EPR signal of GO-1 originates from single-electron carbon radicals, which are temporarily stabilized by the  $\pi$ -conjugated double bonds.

Meanwhile, GO-1 displays a single EPR line without further splitting fingers. In general, the number of EPR lines for a radical can be described by  $n = (2MI + 1)$ , where  $M$  and  $I$  are the numbers of nucleus and spin equivalents, respectively. The single EPR line suggests that there is no equivalent nucleus that is directly bonded to the radicals. Therefore, it is clear that the EPR line originates from the carbon radicals centered at the  $\pi$ -network plane rather than other possible radicals. The formation mechanism of carbon radicals at GO-

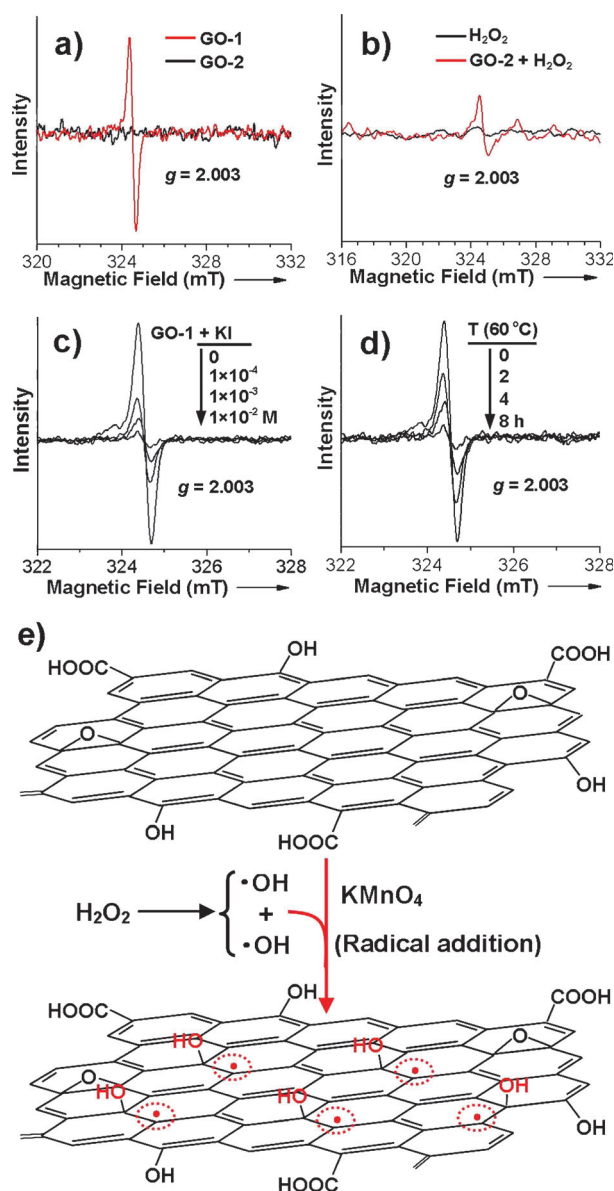


**Figure 3.** a) The EPR spectra of GO-1 and GO-2 (the concentrations are  $0.024 \text{ mg mL}^{-1}$ ). b) The EPR spectra of  $\text{H}_2\text{O}_2$  and the mixture of  $\text{H}_2\text{O}_2$  and GO-2 ( $0.24 \text{ mg mL}^{-1}$ ). c) Evolution of the EPR spectrum of GO-1 ( $0.24 \text{ mg mL}^{-1}$ ) upon addition of KI solutions with different concentrations. d) The time-dependent evolution of the EPR spectrum of GO-1 ( $0.24 \text{ mg mL}^{-1}$ ) at an elevated temperature of 60 °C. The EPR spectra of GO-1 and GO-2 were measured in solution. e) The proposed mechanism for the formation of  $\pi$ -conjugated carbon radicals by the addition of hydroxyl radicals.

1 is illustrated in Figure 3e. In step 4 (see Figure 1a), excess  $\text{H}_2\text{O}_2$  may decompose to  $\cdot\text{OH}$  radicals in the presence of  $\text{KMnO}_4$ . Similar to the addition reaction occurring with many radical scavengers,<sup>[21]</sup> the  $\cdot\text{OH}$  radicals immediately add to the double bonds at the GO plane, leading to the formation of  $\pi$ -conjugated carbon radicals. According to the above-shown data obtained by iodometric titration, the density of carbon radicals at GO-1 is  $2.18 \text{ mmol g}^{-1}$ . Chemiluminescence tests revealed that the density of radicals increased with the



employed  $\text{H}_2\text{O}_2$  amount (Figure S11), and reached the maximum of  $2.18 \text{ mmol g}^{-1}$  at  $1.5 \text{ mL H}_2\text{O}_2$ .

As the carbon radicals are located at the  $\pi$ -network plane, the single electron is likely to conjugate with the  $\pi$  electrons at neighboring double bonds. The single electron is mobile among the conjugated  $\text{C}=\text{C}$  bonds, significantly prompting its oxidizing capability and the efficiency of reactions with the target molecules adsorbed on the basal plane of GO-1. Figure 4a illustrates the mechanism of initiating the ultra-strong chemiluminescence of luminol by the  $\pi$ -conjugated carbon radicals of GO-1. The chemiluminescence experiment is performed in aqueous NaOH, in which the luminol molecule is first transformed into the luminol dianion. The

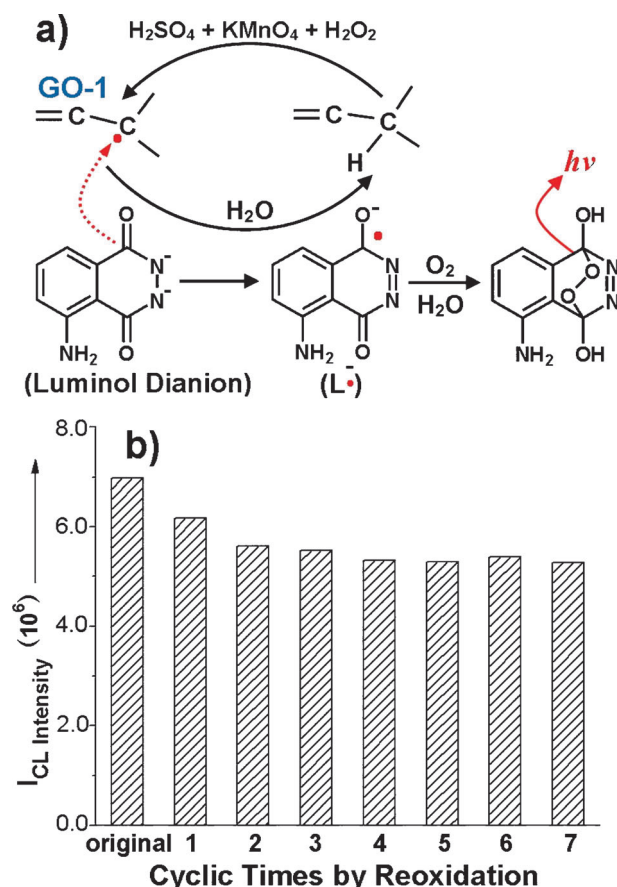


**Figure 4.** a) The mechanism of the chemiluminescence of luminol triggered by the  $\pi$ -conjugated carbon radicals of GO-1. b) The cyclic use of GO-1 to trigger the chemiluminescence after the re-treatment of used GO-1 with  $\text{H}_2\text{O}_2$  in the presence of  $\text{KMnO}_4$  and  $\text{H}_2\text{SO}_4$ .

luminol dianion is then oxidized by the oxidative reagents to produce chemiluminescence. Here, the activated luminol species is adsorbed onto the surface of GO-1 nanosheets by the  $\pi$ - $\pi$  interaction between its benzene ring and the aromatic plane of GO-1. Similar to the  $\pi$ -cationic radicals of HRP,<sup>[19]</sup> a  $\pi$ -conjugated carbon radical of GO-1 attacks the luminol dianion species, and then abstracts a single electron from the carbon-oxygen double bond of the luminol dianion to form a luminol anion radical. Subsequently, a high energy intermediate with an oxygen bridge is produced in the presence of

oxygen and  $\text{H}_2\text{O}$ , and its rapid decomposition leads to the strong chemiluminescence. At the same time, the  $\pi$ -conjugated carbon radical is transformed into a  $\text{C}-\text{H}$  bond by abstracting an  $\text{H}^+$  from  $\text{H}_2\text{O}$ .

The radical oxidation mechanism for chemiluminescence can be further confirmed by the regeneration of the carbon radicals of GO-1 and the cyclic employment in triggering chemiluminescence. The reacted GO-1 was separated by centrifugation, and re-treated with  $\text{H}_2\text{O}_2$ ,  $\text{KMnO}_4$ , and  $\text{H}_2\text{SO}_4$  (Figure 4a). After purification, the product again triggered the strong chemiluminescence of luminol (Figure 4b). When the above-demonstrated process was repeated for seven times, the chemiluminescence intensity was slightly reduced compared to the original one. Meanwhile, an identical EPR signal could also be monitored in the re-treated GO-1 (Figure S12), indicating the regeneration of carbon radicals. Therefore, this offers convincing evidence for the presence of carbon radicals and the radical mechanism, which triggers the chemiluminescence.

In summary, the current work provides a novel understanding of the reaction mechanism for the synthesis of graphene oxide and new insight into its chemical structure and properties. Hydrogen peroxide reacts with graphene oxide by the addition of hydroxyl radicals to the double bonds of the disrupted  $\pi$ -network plane of graphene oxide, leading to the formation of a large number of  $\pi$ -conjugated carbon radicals. The carbon radicals are temporarily stabilized by the  $\pi$ -conjugated double bonds and thus exhibit a strong non-splitting EPR signal. In contrast to previously reported results, the  $\pi$ -conjugated carbon radicals directly initiate the long-lasting, visible chemiluminescence of luminol, which is even stronger than that triggered by horseradish peroxidase. Moreover, the radicals at graphene oxide can be regenerated by re-treatment with hydrogen peroxide and reused for the initiation of the chemiluminescence of luminol, similar to horseradish peroxidase. We thus envision that, with the new understanding, the use of graphene oxide will be extended to other fields including the removal and degradation of organic pollutants and the application as bactericides and disinfectants.

## Experimental Section

Graphene oxide was synthesized according to the widely adopted method.<sup>[18]</sup> The oxidation equivalent of GO-1 was measured by using KI and  $\text{Na}_2\text{S}_2\text{O}_3$  through iodometric titration. Chemiluminescence experiments include chemiluminescence measurements, the observation of visible chemiluminescence, re-treatment of GO-1, and the cycling of chemiluminescence initiation. All above-shown experiments are detailed in the Supporting Information.

Received: May 15, 2014

Revised: June 21, 2014

Published online: July 30, 2014

**Keywords:** carbon radicals · chemiluminescence · graphene oxide · radical reactions

- [1] D. A. Dikin, S. Stankovich, E. J. Zimney, R. D. Piner, G. H. B. Dommett, G. Evmenenko, S. T. Nguyen, R. S. Ruoff, *Nature* **2007**, *448*, 457.
- [2] Y. W. Zhu, S. Murali, W. W. Cai, X. S. Li, J. W. Suk, J. R. Potts, R. S. Ruoff, *Adv. Mater.* **2010**, *22*, 3906.
- [3] X. S. Du, M. Xiao, Y. Z. Meng, A. S. Hay, *Synth. Met.* **2004**, *143*, 129.
- [4] N. A. Kotov, I. Dékány, J. H. Fendler, *Adv. Mater.* **1996**, *8*, 637.
- [5] M. Hirata, T. Gotou, M. Ohba, *Carbon* **2005**, *43*, 503.
- [6] Q. S. Mei, Z. P. Zhang, *Angew. Chem. Int. Ed.* **2012**, *51*, 5602; *Angew. Chem.* **2012**, *124*, 5700.
- [7] Q. S. Mei, K. Zhang, G. J. Guan, B. H. Liu, S. H. Wang, Z. P. Zhang, *Chem. Commun.* **2010**, *46*, 7319.
- [8] Q. Liu, J. B. Shi, J. T. Sun, T. Wang, L. X. Zeng, G. B. Jiang, *Angew. Chem. Int. Ed.* **2011**, *50*, 5913; *Angew. Chem.* **2011**, *123*, 6035.
- [9] a) Y. J. Song, K. G. Qu, C. Zhao, J. S. Ren, X. G. Qu, *Adv. Mater.* **2010**, *22*, 2206; b) D. W. Boukhvalov, D. R. Dreyer, C. W. Bielawski, Y. W. Son, *ChemCatChem* **2012**, *2*, 1844; c) D. R. Dreyer, H. P. Jia, C. W. Bielawski, *Angew. Chem. Int. Ed.* **2010**, *49*, 6813; *Angew. Chem.* **2010**, *122*, 4905; d) D. R. Dreyer, C. W. Bielawski, *Chem. Sci.* **2011**, *2*, 1233.
- [10] B. Brodie, *Ann. Chim. Phys.* **1855**, *45*, 351.
- [11] U. Hofmann, R. Holst, *Ber. Dtsch. Chem. Ges.* **1939**, *72*, 754.
- [12] G. Ruess, *Monatsh. Chem.* **1946**, *76*, 381.
- [13] W. Scholz, H. P. Boehm, *Z. Anorg. Allg. Chem.* **1969**, *369*, 327.
- [14] T. Nakajima, A. Mabuchi, R. Hagiwara, *Carbon* **1988**, *26*, 357.
- [15] A. Lerf, H. He, M. Forster, J. Klinowski, *J. Phys. Chem. B* **1998**, *102*, 4477.
- [16] a) C. H. Lu, H. H. Yang, C. L. Zhu, X. Chen, G. N. Chen, *Angew. Chem. Int. Ed.* **2009**, *48*, 4785; *Angew. Chem.* **2009**, *121*, 4879; b) J. S. Lee, H. A. Joung, M. G. Kim, C. B. Park, *ACS Nano* **2012**, *6*, 2978.
- [17] G. Eda, Y. Y. Lin, C. Mattevi, H. Yamaguchi, H. A. Chen, I. S. Chen, C. W. Chen, M. Chhowalla, *Adv. Mater.* **2010**, *22*, 505.
- [18] W. S. Hummers, R. E. Offeman, *J. Am. Chem. Soc.* **1958**, *80*, 1339.
- [19] H. P. Misra, P. M. Squatrito, *Arch. Biochem. Biophys.* **1982**, *215*, 59.
- [20] T. Szabó, O. Berkesi, P. Forgó, K. Josepovits, Y. Sanakis, D. Petridis, I. Dékány, *Chem. Mater.* **2006**, *18*, 2740.
- [21] K. P. Madden, H. Taniguchi, *J. Phys. Chem.* **1996**, *100*, 7511.